Journal of Materials Chemistry C

ROYAL SOCIETY OF CHEMISTRY

PAPER

Cite this: J. Mater. Chem. C, 2025, 13, 21936

From polyanions to infinite chains: chemical bonding evolution in AX_3 polyhalides under pressure

Enrico Bandiello, †[a] Álvaro Lobato, †*[b] Fernando Izquierdo, †[b] Hussien H. Osman, [acd] Alfonso Muñoz, [e] Plácida Rodríguez-Hernández [e] and Francisco Javier Manjón *[a]

Received 17th April 2025,
Accepted 18th September 2025

DOI: 10.1039/d5tc01566a

rsc.li/materials-c

Polyhalides are molecular systems that defy conventional views of chemical bonding, with infinite linear halide chains being the most challenging systems. By studying CsI_3 under compression, we show how I_3^- polyanions, with electron-rich multicenter bonds, undergo progressive pressure-induced polymerization giving rise to infinite linear iodine chains, I_∞, and demonstrate that these chains, and, by extension, infinite linear halide chains, feature electron-deficient multicenter bonds that are in good agreement with the recently published unified theory of multicenter bonding. This result is in sharp contrast with previous assumptions that considered electron-deficient multicenter bonds to be impossible in valence electron-rich elements such as halogens. The pressure-induced formation of these unconventional bonds explains the decrease of the bandgap and the increase in electrical and photoelectrical conductivity in AX_3 polyhalides under compression.

Introduction

Polyhalides are molecular systems that challenge conventional views of chemical bonding. Their electronic structures have created debates about the hypervalent nature of the halide atoms and challenged the applicability of Lewis diagrams.[1–9] Moreover, they present a wide range of structural arrangements that exhibit a fascinating interplay of covalent, ionic, and metallic properties, allowing them to act as versatile building blocks in molecular electronics, energy storage systems, and photonic materials.[10–15]

Among the many types of polyhalides, infinite linear halide chains, X_∞, stand out as some of the most interesting and rare ones. First proposed by Colin and Gaultier de Claubry, and independently by Stromeyer over two centuries ago in a starch–iodine blue complex,[16,17] the existence of these structures remained theoretical for a long time. In 2013, the first infinite linear halide chain was reported in the $Pm\bar{3}n$ phase of $NaCl_3$, with high-pressure (HP) conditions necessary for its synthesis.[6] It was only in 2016 that a room-pressure (RP) infinite linear iodine chain was synthesized and experimentally verified in a pyrroloperylene–iodine compound for the first time.[18] Since then, many halide-containing compounds have been predicted and found to exhibit this linear atomic arrangement, particularly in nanometrically confined materials and/or under HP conditions.[18–30]

Remarkably, infinite linear atomic chains are not limited to halides;[6,31–33] similar chains have been predicted and observed at both RP and HP in pseudo-halide atoms, such as P^{2-}, Sb^{2-}, Se^-, and Te^-.[34–41] These findings highlight the significance of infinite linear atomic chains as common yet understudied motifs in halide and pseudo-halide chemistry.

Despite the existence of infinite linear halide and pseudo-halide chains, the bonding in these chains remains poorly understood.[19,25,28,33] Even the most studied case, the infinite linear iodine chain, I_∞, challenges conventional models used to describe these systems. Unlike typical polyiodide frameworks composed of donor–acceptor interactions between I_2, I^-, and I_3^- units,[4] the I_∞ chain features equidistant iodine atoms with equivalent charges, making them difficult to ascribe to these models. A simple electron count yields a total of 7 electrons per

[a] Instituto de Diseño para la Fabricación y Producción Automatizada, MALTA Consolider Team, Universitat Politècnica de València, Cno. De Vera, s/n, 46022, València, Spain. E-mail: fjmanjon@fis.upv.es
[b] Departamento de Química Física, MALTA Consolider Team, Universidad Complutense de Madrid, Avda. Complutense, s/n, 28040, Madrid, Spain. E-mail: a.lobato@ucm.es
[c] Instituto de Ciencia de los Materiales de la Universitat de València, MALTA Consolider Team, Universitat de València, Cno. De Vera, s/n, 46022, València, Burjassot, Spain
[d] Chemistry Department, Faculty of Science, Helwan University, 11795 Cairo, Egypt
[e] Departamento de Física, Facultad de Física, MALTA Consolider Team, Universidad de La Laguna, C/. Astrofísico Francisco Sánchez, s/n, 38206, La Laguna, Tenerife, Spain
† These authors contributed equally to this work.

atom in I_∞, thus exhibiting formally two-center one-electron (2c–1e) bonds.[4,42] This electron count suggests that the electronic structure of I_∞, as well as other infinite linear halide and pseudo-halide chains, features half-filled bands,[43,44] resembling the fascinating metallic 1D conductors with electron-deficient bonds, such as the infinite linear hydrogen chain.[45,46]

The delocalized bonding perspective of infinite linear halide chains clashes with the generally accepted view that valence electron-rich elements (groups 15 to 18) primarily favor covalent bonding or electron-rich multicenter bonds (ERMBs), also known as three-center–four electron (3c–4e) bonds, hypervalent bonds, or hyperbonds.[42,47] In this classical view, it is also believed that electron-deficient multicenter bonds (EDMBs), also known as three-center–two-electron (3c–2e) bonds, could only occur in valence electron-deficient elements (*e.g.*, hydrogen and groups 1, 2, and 13).[48]

The conventional view of chemical bonding exposed in the preceding paragraph has recently been challenged by a unified theory of multicenter bonding, which explains the origin and formation process of ERMBs and EDMBs and their relationship with classical primary bonding (covalent, ionic, and metallic) and also with classical secondary non-covalent bonding (van der Waals and hydrogen bonding).[49,50] In this article, we aim to explore the chemical bonding and electronic delocalization within infinite linear halide and pseudo-halide chains. For this purpose, we have performed a joint HP experimental and theoretical study on the compound CsI_3. It is well known that HP conditions modify the chemical properties of the elements and induce remarkable changes in the chemistry of materials.[51–53] The ability of pressure to continuously modify the interatomic distances enables us to track the evolution of chemical bonding in a continuous way that would not be possible by comparing different compounds (atomic substitution) or by reducing the system, as already explained in the unified theory of multicenter bonding.[50] This is consistent with the view of Burdett that pressure could be used to study infinite linear chains by overcoming the typical Peierls distortion in these chains.[45] For this purpose, we have selected CsI_3 because it is one of the AX_3 halides that exists at RP[54–58] and forms I_∞ chains at HP.[6,19–25] CsI_3 can be considered a test bed model for the other AX_3 halides (A = Li, Na, K, Rb, Tl, and NH_4; X = F, Cl, Br, and I) and exhibits X_∞ chains at the lowest pressure within the AX_3 family, facilitating their experimental study. Details of experimental measurements and theoretical calculations can be found in sections 1 and 2 of the supplementary information (SI).

Our work demonstrates that pressure induces the formation of infinite linear halide chains in the cubic $Pm\bar{3}n$ HP phase of AX_3 halides and that the bonding in that chain is the EDMB, thereby revealing the bonding nature of infinite linear halide and pseudo-halide chains. Such a finding confirms that valence electron-rich elements can exhibit EDMBs in infinite linear atomic chains. This demonstration opens new avenues for designing materials with strong optical absorption, photovoltaic applications, thermoelectric properties, and data storage associated with this kind of unconventional bonding.[59] Moreover, the pressure-induced process of formation of EDMBs in the infinite linear chains in CsI_3 at HP fully agrees with the recently published unified theory of multicenter bonding.[49,50]

Results and discussion

X-ray diffraction (XRD) measurements at RP allowed us to confirm that our CsI_3 samples contained only the *Pnma* phase (see Fig. S1 and structural data in Table S1 in the SI). It is known that CsI_3 undergoes the *Pnma* → $P\bar{3}c1$ → $Pm\bar{3}n$ sequence of phase transitions at HP,[22–24] a similar sequence to that of other AX_3 halides.[6,25] The *Pnma* phase features isolated I_3^- anions in a herringbone motif (Fig. 1a); the $P\bar{3}c1$ phase is characterized by linearly aligned I_3^- anions (showing secondary $I_3^-\cdots I_3^-$ interactions) in three perpendicular directions (Fig. 1b); and the $Pm\bar{3}n$ phase exhibits I_∞ chains along the three perpendicular directions (Fig. 1c). All these phases show typical ionic bonds between Cs^+ and I_3^- anions as well as homonuclear bonds between the I atoms themselves. Since the relevant change in chemical bonding occurs alongside the $P\bar{3}c1$ → $Pm\bar{3}n$ phase transition during the polymerization of the I_3^- units to form I_∞ chains, we mainly focus our discussion on these two phases and their phase transition at HP.

We did not perform HP-XRD measurements since they have been carried out in previous works and good data were previously obtained and reported, as discussed below. In particular, previous HP-XRD measurements showed that the

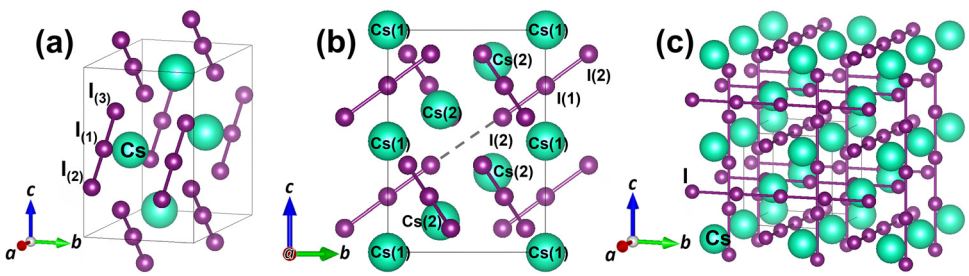

Fig. 1 Details of the crystalline structure of the *Pnma* (a), $P\bar{3}c1$ (b), and $Pm\bar{3}n$ (c) phases in CsI_3 at 0, 2, and 24 GPa, respectively. Cs, I(1), I(2), and I(3) indicate the four independent atoms in the *Pnma* phase. Cs(1), Cs(2), I(1), and I(2) indicate the four independent atoms in the $P\bar{3}c1$ phase. I(1) and I(2) are the central and external atoms of the I_3^- units. The dashed line in the $P\bar{3}c1$ phase indicates the intermolecular bonding ($I_3^-\cdots I_3^-$) between aligned I_3^- units. In the $Pm\bar{3}n$ phase, there is only one Cs and one I independent atoms.

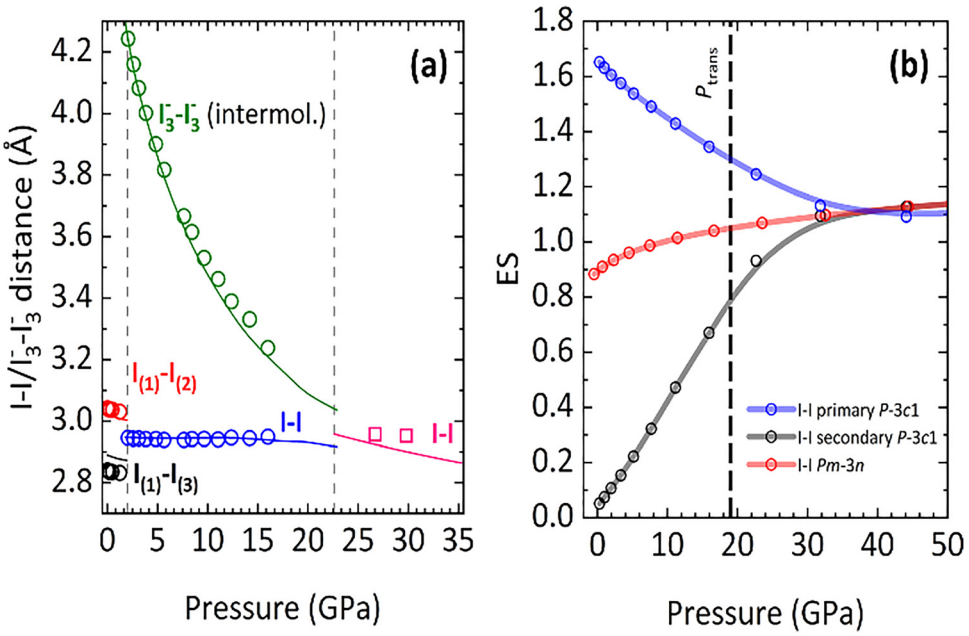

Fig. 2 (a) Pressure dependence of the experimental (symbols) and theoretical (lines) primary (intramolecular $I_{(1)}$–$I_{(2)}$, $I_{(1)}$–$I_{(3)}$, and I–I) and secondary (intermolecular I_3^-–I_3^-) bond distances in CsI_3. Experimental values in (a) are taken from ref. 22 and 23. Dashed vertical lines indicate the experimental phase transition pressures. (b) Pressure dependence of the calculated number of electrons shared (ES) in the bonds of the $P\bar{3}c1$ and $Pm\bar{3}n$ phases in CsI_3. ES values of the $I_{(1)}$–$I_{(2)}$ and $I_{(1)}$–$I_{(3)}$ bonds in the *Pnma* phase are not shown to avoid misunderstanding. Bold lines in (b) are a guide for the eye. The vertical dashed line indicates the theoretical phase transition pressure.

Pnma → $P\bar{3}c1$ phase transition in CsI_3 occurs at very low pressures (*ca.* 1.0 GPa) and that the $P\bar{3}c1$ → $Pm\bar{3}n$ phase transition takes place at *ca.* 22.6 GPa.[22–24] These values agree with our *ab initio* calculations (Fig. S2 in the SI) and Raman measurements (Fig. S5–S11 in the SI). Moreover, our theoretical values for the unit cell volume, lattice parameters, atomic parameters, and I–I bond lengths in the three phases agree with experimental values[23] (see Tables S1–S3 in the SI) and previous calculations on CsI_3.[19,22–24] Furthermore, our simulated results accurately reproduce the experimental pressure dependence of the unit cell volume in the three phases (Fig. S3 and Table S4 in the SI) and of the interatomic bond distances (Fig. 2a). The good agreement between experimental and simulated results gives us confidence in: (i) the goodness of the experimental structural data previously reported, and (ii) the accuracy of our calculations, which we will use to study the change in chemical bonding in CsI_3 under compression.

Before discussing the chemical bonding between the I atoms in the different crystalline phases of CsI_3, we need to comment on the pressure dependence of the I–I bond distances in these phases (Fig. 2a). The *Pnma* phase has two main I–I distances, $I_{(1)}$–$I_{(2)}$ and $I_{(1)}$–$I_{(3)}$, corresponding to the two bonds of the asymmetric I_3^- polyanion. They exhibit an expected decrease with increasing pressure, leading to a decrease in the total length of the I_3^- polyanion (see discussion in section 3.1 of the SI). On the other hand, the $P\bar{3}c1$ phase features a symmetric I_3^- polyanion with a short (primary) intramolecular I–I (I(1)–I(2)) bond length of 2.945 Å at *ca.* 2.0 GPa.[12] In addition, we have to consider a long (secondary) intermolecular I–I bond distance that corresponds to the intermolecular $I_3^-\cdots I_3^-$ (I(2)–I(2)) interaction between the external I atoms of neighbouring I_3^- polyanions arranged in a linear fashion (Fig. 1b). Interestingly, while the long secondary intermolecular I–I bond distance of the phase $P\bar{3}c1$ strongly decreases upon compression, a small anomalous increase of the short primary intramolecular I–I bond distance is produced (see Fig. 5 in ref. 23). Importantly, these two distances equalize at HP, leading to the formation of I_∞ chains in the three dimensions in the cubic $Pm\bar{3}n$ phase, as a result of the pressure-induced polymerization (PIP) of the I_3^- units above 22 GPa. There is only a single I–I bond distance in the I_∞ chains of the cubic phase that shows a normal decrease with increasing pressure (Fig. 2a).

The changes in the I–I bond distances in CsI_3 under compression align with the three stages of the process of multicenter bond formation proposed in the unified theory of multicenter bonding (see discussion in section 3.2 of the SI)[49,50] and closely match the variations observed in the Raman vibrational modes (see discussion in section 4.4 of the SI, Fig. S5–S11 and Tables S5–S9). Regarding the vibrational properties and their relation to chemical bonding, here we just want to emphasize that the short primary bonds in the $P\bar{3}c1$ phase, which exhibit an anomalous increase in bond distance, are associated with the softening of the high-wavenumber vibrational modes (related to stretching vibrations).[49,50] The soft behavior of these modes in the $P\bar{3}c1$ phase is followed by their hardening in the $Pm\bar{3}n$ phase. This hardening is linked to the normal compression of the symmetric I–I bonds in the I_∞ chains above 22 GPa, as already pointed out. In summary, the

sequence of equalization of the primary and secondary bond distances along with the anomalous increase of the short primary bond length and the softening of vibrational modes in the $P\bar{3}c1$ phase, is characteristic of stage 2 (in which the multicenter interaction appears) in the process of formation of multicenter bonds.[49,50] This process culminates upon reaching the $Pm\bar{3}n$ phase, with the formation of multicenter bonds in I_∞ chains (stage 3).[49,50] At this point, we note that it is difficult to determine, relying only on the interatomic distances and vibrational data under compression, whether the bonds in I_∞ chains are EDMBs or ERMBs.

In this regard, it has been suggested that the homonuclear bonds in some infinite linear atomic chains, such as P–P bonds in infinite linear P^{2-} chains in the HP phase of Mo_2P[39] and Se–Se bonds in infinite linear Se^- chains in the HP phase of YSe_3,[40] are 2c–1e bonds (see the discussion of these bonds in relation to I–I bonds in I_∞ in CsI_3 in section 3.3 of the SI). More recently, Te–Te bonds in infinite linear Te^- chains, Te_∞^-, in TlTe at RP, as well as in I_∞, have been classified as EDMBs;[4,49,50,58] however, to the best of our knowledge, no proof of the multicenter character of bonding in infinite linear atomic chains has been provided for any compound. Up to now, we have just shown that the trend in I–I bond distances and vibrational properties (see section 4.4 of the SI) under compression in the $P\bar{3}c1$ phase of CsI_3 supports the multicenter character of symmetric I–I bonds in I_∞ in the $Pm\bar{3}n$ phase, according to the unified theory of multicenter bonding.[49,50] Hereon, we will focus on confirming the multicenter character of bonding in I_∞ with other bonding descriptors and also on determining the ERMB or EDMB nature of the bonds in I_∞ with the help of Fig. 2b.

According to the unified theory of multicenter bonding,[49,50] the distinction between ERMBs and EDMBs can be made by calculating the number of electrons shared (ES) and the normalized number of electrons transferred (ET) between two atoms using the density-based quantum theory of atoms in molecules (QTAIM)[60] (see details of these calculations in section 2 of the SI). In this density-based method, the ES value is derived as twice the delocalization index (DI) calculated between two atoms. While ERMBs usually feature ES values higher than 1.4 and ET values higher than 0.2, EDMBs usually exhibit ES values around 1.0 for ET = 0 and smaller values if ET $\neq$ 0.[50]

It is well known that the X–X bonds within the X_3^- anions in the *Pnma* and $P\bar{3}c1$ phases of AX_3 halides are ERMBs, *i.e.* three-center–four-electron (3c–4e) bonds.[19,22,24,25,50] This is confirmed by our calculated ES (1.66) and ET (0.32) values for the short primary (intramolecular) I–I bond at 0 GPa in the $P\bar{3}c1$ phase of CsI_3, which are comparable to those of the isolated I_3^- polyanion.[50] These bonding features change when pressure comes into play (see Fig. 2b, ES and ET values for I–I bonds in the different phases of CsI_3 are shown in Table S10 of the SI). Upon compression, the ES values of both intramolecular and intermolecular bonds in the $P\bar{3}c1$ phase evolve inversely to the bond distances (Fig. 2b). While the short (long) intramolecular (intermolecular) bond distance increases (decreases), the corresponding ES value decreases (increases). This result indicates that as the short intramolecular bond lengthens, it loses electronic charge, whereas the long intermolecular bond gains electronic charge as it shortens. The overall process leads to an equalization of both I–I bond distances and ES values (around 1.1) in the $Pm\bar{3}n$ phase. In this context, the equalization of ES values gives further support to the multicenter character of the I–I bonds in I_∞.[49,50] Moreover, the ES value for the equalized I–I bonds in I_∞ is characteristic of EDMBs, indicating delocalized electron-deficient bonding in I_∞, in good agreement with previous suggestions.[4,49,50]

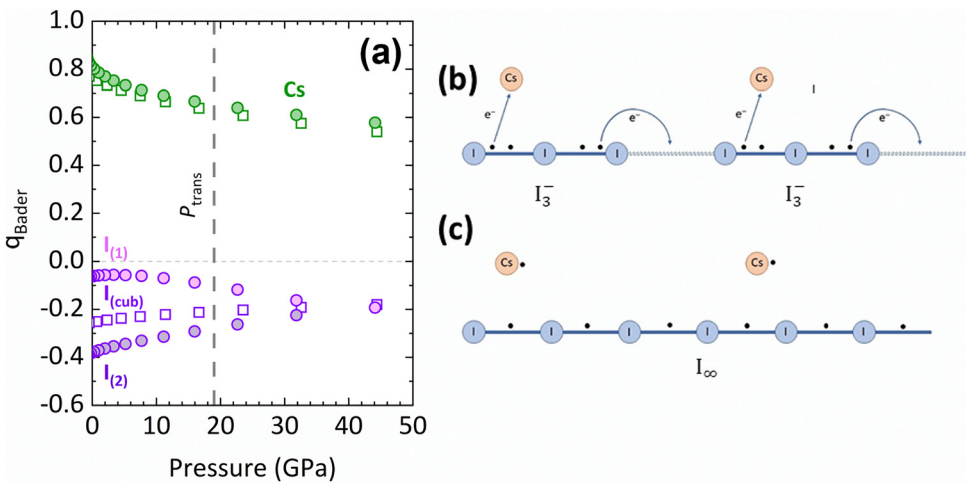

Fig. 3 (a) Pressure dependence of the Bader charges (q_{Bader}) of the average Cs and individual I atoms in the $P\bar{3}c1$ (full circles) and $Pm\bar{3}n$ (open squares) phases of CsI_3. $I_{(1)}$ and $I_{(2)}$ indicate the central and the terminal atoms of the I_3^- anion in the $P\bar{3}c1$ phase, respectively; $I_{(cub)}$ indicates the iodine atoms in I_∞ in the $Pm\bar{3}n$ phase. (b) Scheme of the charge transfer processes taking place in the $P\bar{3}c1$ phase at HP. The ERMB at the I_3^- polyanion exhibits two electrons between each pair of I atoms, but not equally distributed and shared, as explained in the unified theory of multicenter bonding.[50] Electrons are transferred from the I_3^- units to the Cs atom and also to the intermolecular bond as I_3^- polyanions approach each other. (c) Scheme of interatomic bonding at the $Pm\bar{3}n$ phase. EDMBs at I_∞ feature a single electron between each pair of I atoms.

Bader charges calculated with QTAIM (Fig. 3a and Table S11 in the SI) allow us to determine the ET values of the I–I bonds (Table S9 in the SI), which also provides information on the change of I–I chemical bonding under compression. In the $P\bar{3}c1$ phase near RP, the average Cs atom shows a near +1 charge, while the I_3 unit carries a negative charge, consistent with the behavior of a monovalent alkali cation and an anion with a nominal charge –1, respectively. Specifically, the central I atom of the I_3^- polyanion at RP has a small Bader charge (*ca.* –0.07e), while the terminal I atoms have almost a –0.38e value. This result means that the terminal iodine atoms, I(2), share most of the electronic charge (0.83e) donated by the Cs cation. This accumulation of negative charge on the terminal I atoms is characteristic of the I_3^- polyanion and is a feature of ERMBs, as already discussed for this polyanion and other molecules with ERMBs, such as XeF_2 and HF_2^-.[50]

With increasing pressure, the Bader charge of the Cs atom decreases from *ca.* +0.83e in the $P\bar{3}c1$ phase to *ca.* +0.6e upon reaching the $Pm\bar{3}n$ phase at 22 GPa (Fig. 3a). This indicates that under compression, the I_3^- polyanion returns part of the electronic charge received from the Cs atom at RP; a behavior previously noted in *ab initio* calculations of CsI_3 at HP.[19,23] This process is also accompanied by a decrease in the Bader charge difference between the central and external I atoms of the I_3^- polyanion in the $P\bar{3}c1$ phase, resulting in a gradual decrease of the ET value for the primary I–I bonds in the $P\bar{3}c1$ phase from 0.32 near RP to 0.2 at 19 GPa. This trend culminates in a zero ET value for the symmetric I–I bond in I_∞ in the $Pm\bar{3}n$ phase, where all I atoms occupy the same Wyckoff site, further supporting our previous ES analysis and confirming that the bonding in the I_∞ chain should be considered as formed by an array of collinear (2c–1e) EDMBs or equivalently a concatenation of linear 3c–2e bonds.[49,50] In fact, the ES value of the I–I bonds in the $Pm\bar{3}n$ phase is slightly above 1 because the charge of each I atom in the I_∞ chain is not zero but *ca.* −0.2e above 22 GPa (the Bader charge of each I atom in the $Pm\bar{3}n$ phase). This means that there is an electronic charge of *ca.* 7.2e per iodine atom and *ca.* 1.2e per I–I bond in the I_∞ chain around 22 GPa (smaller values at higher pressures). Note that the other six electrons of each I atom in the I_∞ chain are located in three lone electron pairs located in the plane perpendicular to the chain (not plotted in Fig. 3c), as corresponds to the A(0,3,1) multicenter unit (see Fig. 10 in ref. 50).

The joint evolution of the calculated ES and ET values of the short (primary) I–I bond in the $P\bar{3}c1$ phase with increasing pressure allows us to monitor the pressure-induced change in chemical bonding from ERMB in I_3^- to EDMB in I_∞, as shown in the ES *vs.* ET map (Fig. 4). The data reveal that the primary I–I bond in the $P\bar{3}c1$ phase shifts from the ERMB region near RP towards the EDMB region as the $Pm\bar{3}n$ phase is reached at HP. This ERMB → EDMB chemical bonding transition seems to occur due to the charge depletion at the I_3^- polyanion. In contrast to previous calculations,[19,23] our results indicate that there are two mechanisms by which the polyanion charge is reorganized during the process of PIP of the I_3^- units in the $P\bar{3}c1$ phase. First, a small fraction of the charge of the I_3^- polyanions is returned to the Cs atoms, as shown by the Bader charges (Fig. 3a). Second, an important fraction of the electronic charge of the I_3^- polyanions is transferred from the intramolecular bonds to the intermolecular $I_3^-\cdots I_3^-$ interactions as the I_3^- units approach upon compression, as shown by the inverse behavior of the ES values of both bonds (Fig. 2b). This second mechanism has not been commented in previous HP works on AX_3 halides. The two charge-transfer processes are depicted schematically in Fig. 3b for CsI_3. As a consequence of the charge transfer, the I_∞ chain features *ca.* one electron shared between every two iodine atoms, *i.e.* a 2c–1e EDMB, as previously suggested for I_∞ and infinite linear Te^- chains in TlTe at RP.[4,50,58] This result is consistent with the 2c–1e bonds predicted in P^{2-} and Se^- atoms in MoP_2 and YSe_3 at HP, respectively.[39,40] Therefore, we can conclude that the P–P and Se–Se bonds along the P_∞ and Se_∞ chains in these compounds are also EDMBs.

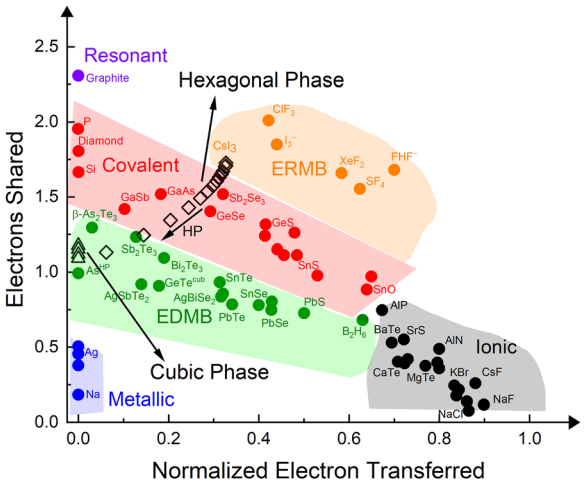

Fig. 4 ES *vs.* ET map showing the evolution of the calculated ES and ET values of the hexagonal $P\bar{3}c1$ phase (black rhombuses) at different pressures until the cubic $Pm\bar{3}n$ phase (black triangles) is attained above 19 GPa.

Once the EDMB nature of bonding in I_∞ has been clarified using a density-based method as QTAIM, we want to stress that the change in chemical bonding can also be traced with an orbital-based method (see details in section 2 in the SI). Within the orbital-based analysis with the LOBSTER software,[61,62] the ES value is obtained as twice the two-center integrated crystal orbital bond index, ICOBI(2c), and the normalized ET value is obtained from the Löwdin charge. The ICOBI(2c) values for the short primary and long secondary I–I bond distances in the $P\bar{3}c1$ phase (Fig. S12 in the SI) show the same behavior as the ES, reinforcing that both the density-based and orbital-based analyses point towards the EDMB nature in the I_∞ chain.

The multicenter character of I_∞ is further supported by the integrated crystal orbital bond index for three centers, ICOBI(3c), which is the only known multicenter bond index available for solids, to our knowledge. Fig. 5a shows how the ICOBI(3c) for the I–I–I bond in the I_3^- polyanion of the $P\bar{3}c1$ phase changes under compression. It changes from *ca.* −0.4 in the $P\bar{3}c1$ phase at RP—a value typical of the isolated I_3^-

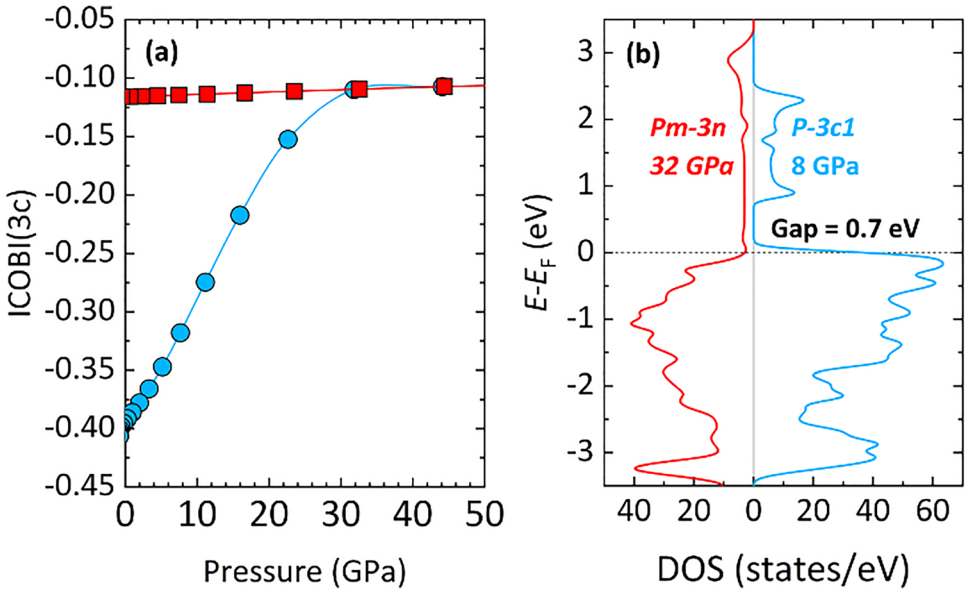

Fig. 5 (a) Pressure dependence of ICOBI(3c) in the I_3^- units of the $P\bar{3}c1$ phase (blue circles) and in the infinite linear iodine chain of the $Pm\bar{3}n$ phase (red squares). (b) Electronic density of states (DOS) for the $P\bar{3}c1$ ($Pm\bar{3}n$) phase at 8 GPa (32 GPa).

polyanion and XeF_2—[49,50,62–64] to −0.1 in the $Pm\bar{3}n$ phase. This last value is similar to that found for the octahedrally-coordinated phases of pnictogens, chalcogens, and phase change materials, such as rocksalt-like β-GeTe and PbTe, *i.e.* systems with EDMBs.[49,50,65] While previous studies have interpreted negative ICOBI(3c) values as indicative of ERMBs,[62–64] our results suggest that a value close to −0.1 is indicative of the presence of EDMBs. This conclusion is supported by the charge depletion and the PIP of I_3^- units in CsI_3, which aligns with the chemical picture of 2c–1e bonds, as confirmed by ELF analysis in other AX_3 halides.[25]

We propose that the negative value of ICOBI(3c) for the I–I bonds in I_∞ is consistent with EDMB formation, considering I_∞ as a resonant form (electron fluctuation) that accumulates charge with respect to the average population, as recently demonstrated by analyzing the statistics of the electron distributions.[66] In the I_∞ chain, the two resonant forms with alternating bonds (see Fig. 6) may act as charge reservoirs, potentially explaining its negative ICOBI(3c) value. To the best of our knowledge, this is the first report of bonding evolution from ERMBs to EDMBs in a material. Our findings underscore the role of pressure in resolving bonding controversies, such as the ones related to ERMBs and EDMBs.

The pressure-induced change in chemical bonding from ERMBs to EDMBs in CsI_3 correlates with the change in the electrical and photoelectrical properties of the material as experimentally measured,[19,23–25] and as shown by the electronic density of states (Fig. 5b). The hexagonal *Pnma* phase at 0 GPa is a semiconductor with an experimental bandgap of almost 1.79 eV.[67] Our calculations show that the bandgap at 8 GPa in the $P\bar{3}c1$ phase reduces to *ca.* 0.7 eV and the cubic $Pm\bar{3}n$ phase at 30 GPa exhibits no gap. Our calculated pressure-induced decrease of the bandgap is consistent with experimental

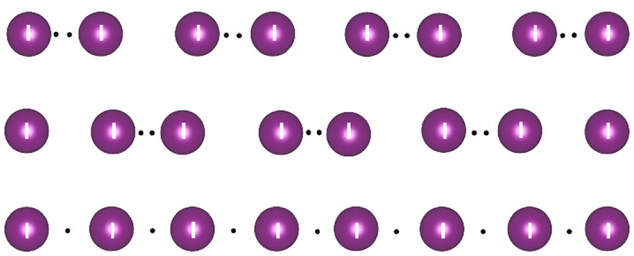

Fig. 6 I_∞ can be considered as concatenated 2c–1e bonds (bottom) but also as a resonant structure of the three above chains. Violet balls represent I atoms and black dots represent the bonding electrons between the atoms.

results.[24] Moreover, our calculations show that the cubic $Pm\bar{3}n$ has quasi-metallic conductivity that explains the pressure-induced increase in the electrical conductivity and photoconductivity in the *Pnma* → $P\bar{3}c1$ → $Pm\bar{3}n$ sequence of phase transitions at HP.[19,23–25] The quasi-metallic conductivity of EDMBs in the cubic phase of CsI_3 is typical of semimetals with half-filled bands[43,44,49,50] and is characteristic of phase change materials that are considered incipient metals.[59,65] Moreover, the change in bonding agrees with the change in the electronic properties previously observed in similar pseudo-halide systems[34–41] and is consistent with the electrical properties found in starch–iodine and pyrroloperylene–iodine complexes exhibiting infinite linear iodine chains.[18]

We would like to finish by commenting on the optical properties of CsI_3 under compression. The experimentally measured decrease of the bandgap of CsI_3 with increasing pressure[24] is consistent with the increase of the calculated optical dielectric constant, ε_∞, in the $P\bar{3}c1$ phase, as shown in Fig. S13 in the SI. It is shown that the optical dielectric constant

is quite small (*ca.* 5) near RP when ERMBs are present in I_3^- units and increases in the hexagonal phase up to close to 100. Notably, the optical dielectric constant remains constant around a value close to 80 in the cubic phase above 22 GPa and does not diverge to infinity as expected in a metal. The increase of the optical dielectric constant from RP to 22 GPa explains why the $Pm\bar{3}n$ phase of CsI_3 shows metallic cluster. A feature that is consistent with the EDMB present in the I–I bonds of the $Pm\bar{3}n$ phase, since high values (but not infinite) of the optical dielectric constant and metallic luster have been measured in the phases of incipient metals, such as the simple cubic phase of cubic polonium and arsenic, as well as in the rocksalt phase of phase change materials.[49,65,68] The changes in chemical bonding in CsI_3 under compression are also traced by the increase of the chemical bond polarizability, leading to unusually high Born effective charges in the phase with EDMBs, as shown in Fig. S13. Clearly, the calculated Born effective charges of Cs atoms in the $P\bar{3}c1$ phase show a negligible change with increasing pressure. In contrast, a notable increase of the calculated Born effective charges of I(1) atoms (double than of I(2)) has been obtained upon going from discrete I_3^- units to I_∞ chains. These high values of Born effective charges in the iodine atoms have been also found in the simple cubic phase of polonium and arsenic, as well as in the rocksalt phase of phase change materials, *i.e.*, materials featuring EDMBs.[49,65,68]

Conclusion

We have demonstrated that the pressure-induced $Pnma \rightarrow P\bar{3}c1 \rightarrow Pm\bar{3}n$ sequence of phase transitions in CsI_3 leads to a pressure-induced polymerization (PIP) of the I_3^- units present in the original *Pnma* phase. The PIP drives a change in chemical bonding from ERMBs in discrete I_3^- polyanions (in the *Pnma* and $P\bar{3}c1$ phases) to EDMBs in infinite linear iodine chains, I_∞ (in the $Pm\bar{3}n$ phase). This study confirms that EDMBs, as infinitely extended 2c–1e bonds (or equivalently as concatenated 3c–2e bonds) in one direction, are the characteristic bonding within the X_∞ chains in the $Pm\bar{3}n$ phases of all AX_3 halides. Therefore, this work supports the recent predictions of the presence of EDMBs in infinite linear atomic chains.[4,50,58] In this context, it must be mentioned that a pressure-induced polymerization of IO_3^- units has been recently reported in distorted AIO_3 perovskites leading to the formation of EDMBs in the polymerized units.[69]

Noteworthily, the presence of EDMBs in the X_∞ chains is consistent with the prediction of 2c–1e EDMBs in infinite linear Sb^{2-} and Te^- chains in Li_2Sb and TlTe at RP, respectively,[50] and with the earlier proposals of 2c–1e bonds in infinite linear P^{2-} and Se^- chains in Mo_2P and YSe_3 at HP, respectively.[39,40] This conclusion is reasonable since P^{2-}, Sb^{2-}, Se^-, and Te^- anions are isoelectronic to halide atoms. Consequently, EDMBs in the form of extended 2c–1e bonds are expected to be found not only in infinite linear halide chains but also in infinite linear pseudo-halide chains in many materials, *e.g.*, in infinite linear Se^- and Te^- chains in isostructural β-$ErSe_2$[70] and UTe_2 at RP,[71] respectively, and in the HP *P6/mmm* phase of Sc_2P.[41] The discovery of EDMBs in infinite linear atomic chains and their related quasi-metallic conductivity opens new avenues for designing materials with novel optical, electronic, and optoelectronic properties.

We emphasize that the example of compressed AX_3 halides illustrates that EDMBs do actually occur in valence electron-rich elements, such as halogen atoms. Therefore, this work complements a previous study in which EDMBs were found in pnictogens and chalcogens at different pressures.[49] It is also worth highlighting that the pressure-induced change in chemical bonding in CsI_3 from the $P\bar{3}c1$ phase to the $Pm\bar{3}n$ phase is consistent with: (i) the change from I–I bond elongation to compression; (ii) the change from phonon softening to hardening (in high-wavenumber vibrational modes), and (iii) the change in optical, electronic, and photoelectronic properties between phases with I_3^- and I_∞, as noted in previous HP works on AX_3 halides.[6,19–25] These changes are related to the three-stage process describing the formation of multicenter bonds in the recently formulated unified theory of multicenter bonding.[49,50] This theory challenges our current understanding of chemical bonding in materials and offers insights into important technological materials for enhanced applications.[4,59]

We should finally note that during the finalization of this manuscript, we have been aware of a manuscript which has addressed the nature of chemical bonding in 1D iodine chains in the $[Na(DMSO)_3]_n(I_2)_n$ solid.[72] In that work, authors make a nice historical revision of the 1D iodine chains in different systems, such as the 200 year-old starch–iodine blue complex, leading to a potato stagnation procedure with the KI/I_2 starch test, and herapathite, whose unique optical properties led to the foundation of the Polaroid Corporation. These systems evidence the technological importance of 1D iodine chains, like those found in the $Pm\bar{3}n$ phase of AX_3 polyhalides for possible iodine-based conductors, superconductors, batteries, data storage, and optical materials with strong optical absorption for photovoltaic applications associated with unconventional EDMBs.[59]

Conflicts of interest

There are no conflicts to declare.

Data availability

The data supporting this article have been included as part of the supplementary information (SI). Supplementary information: experimental and theoretical details; structural properties of the three phases of CsI_3 including the discussion of the total bond length of the I_3^- polyanion in different phases of CsI_3, of the three stages of multicenter bond formation in CsI_3 from the point of view of interatomic distances, and the discussion about the electron-deficient multicenter (2c–1e) bonds in

infinite linear atomic chains; vibrational properties of the three phases of CsI_3, including the discussion of the three stages of multicenter bond formation in CsI_3 from the point of view of the vibrational properties; and data for the analysis of the electron density topology.[73–94] See DOI: **https://doi.org/10.1039/d5tc01566a**.

Acknowledgements

This publication is financed by Spanish Ministerio de Ciencia e Innovación (MCIN) and the Agencia Estatal de Investigación MCIN/AEI/10.13039/501100011033 as part of the project MALTA Consolider Team network (RED2022-134388-T), and I + D + i projects PID2021-122585NB-C22 and PID2022-138076NB-C42/C44 co-financed by EU FEDER funds, by project PROMETEO CIPROM/2021/075 (GREENMAT) financed by Generalitat Valenciana and co-financed by EU FEDER. This study also forms part of the Advanced Materials programme supported by MCIN with funding from European Union NextGenerationEU (PRTR-C17.I1) and by Generalitat Valenciana through project MFA/2022/025 (ARCANGEL). We would like to express our gratitude to Giulia Longo for providing us with the experimental XRD patterns of CsI_3 under room temperature conditions and to Matteo Savastano and Ángel Vegas for their insightful and engaging discussions on our findings. Their input and feedback greatly enriched the development of this article.

References

1 P. H. Svensson and L. Kloo, Synthesis, structure, and bonding in polyiodide and metal iodide– iodine systems, *Chem. Rev.*, 2003, **103**, 1649–1684.
2 M. Savastano, Words in supramolecular chemistry: the ineffable advances of polyiodide chemistry, *Dalton Trans.*, 2021, **50**, 1142.
3 M. Savastano, C. Bazzicalupi and A. Bianchi, Novel cyclen-polyiodide complexes: a reappraisal of I–I covalent and secondary bond limits, *Dalton Trans.*, 2022, **51**, 10728.
4 M. Savastano, H. H. Osman, Á. Vegas and F. J. Manjón, Rethinking polyiodides: the role of electron-deficient multicenter bonds, *Chem. Commun.*, 2024, **60**, 12677.
5 K. Sonnenberg, L. Mann, F. A. Redeker, B. Schmidt and S. Riedel, Polyhalogen and Polyinterhalogen Anions from Fluorine to Iodine, *Angew. Chem., Int. Ed.*, 2020, **59**, 5464.
6 W. Zhang, A. R. Oganov, A. F. Goncharov, Q. Zhu, S. E. Boulfelfel, A. O. Lyakhov, E. Stavrou, M. Somayazulu, V. B. Prakapenka and Z. Konopkova, Unexpected stable stoichiometries of sodium chlorides, *Science*, 2013, **342**, 1502.
7 T. Poręba, M. Ernst, D. Zimmer, P. Macchi and N. Casati, Pressure-Induced Polymerization and Electrical Conductivity of a Polyiodide, *Angew. Chem., Int. Ed.*, 2019, **58**, 6625.
8 A. A. Petrov, S. A. Fateev, Y. V. Zubavichus, P. V. Dorovatovskii, V. N. Khrustalev, I. A. Zvereva, A. V. Petrov, E. A. Goodilin and A. B. Tarasov, Methylammonium polyiodides: remarkable phase diversity of the simplest and low-melting alkylammonium polyiodide system, *J. Phys. Chem. Lett.*, 2019, **10**, 5776–5780.
9 C. Wang, D. Danovich, S. Shaik and Y. Mo, Halogen bonds in novel polyhalogen monoanions, *Chem. Eur. J.*, 2017, **23**, 8719.
10 R. Brückner, H. Haller, S. Steinhauer, C. Müller and S. Riedel, A 2D Polychloride Network Held Together by Halogen–Halogen Interactions, *Angew. Chem., Int. Ed.*, 2015, **54**, 15579–15583.
11 H. T. Yua, L. J. Yan, Y. W. He, H. Meng and W. Huang, Unusual Photoconductive Property of Polyiodide and Enhancement by Catenating with 3-Thiophenemethylamine Salt, *Chem. Commun.*, 2017, **53**, 432–435.
12 Z. Yin, Q.-X. Wang and M.-H. Zeng, Iodine Release and Recovery, Influence of Polyiodide Anions on Electrical Conductivity and Nonlinear Optical Activity in an Interdigitated and Interpenetrated Bipillared-Bilayer Metal–Organic Framework, *J. Am. Chem. Soc.*, 2012, **134**, 4857–4863.
13 E. Tanaka and N. Robertson, Polyiodide solid-state dye-sensitized solar cell produced from a standard liquid I–/I3– electrolyte, *J. Mater. Chem. A*, 2020, **8**, 19991–19999.
14 F. Li, C. Zhou, J. Zhang, Y. Gao, Q. Nan, J. Luo, Z. Xu, Z. Zhao, P. Rao, J. Li, Z. Kang, X. Shi and X. Tian, Mullite Mineral-Derived Robust Solid Electrolyte Enables Polyiodide Shuttle-Free Zinc-Iodine Batteries, *Adv. Mater.*, 2024, **36**, 2408213.
15 D. D. Yin, B. Y. Li, L. Y. Zhao, N. Gao, Y. N. Zhang, J. Feng, X. F. Cui, C. H. Xiao, Y. Q. Su, K. Xi, S. J. Ding and H. Y. Zhao, Polymeric Iodine Transport Layer Enabled High Areal Capacity Dual Plating Zinc-Iodine Battery, *Angew. Chem., Int. Ed.*, 2025, **64**, e202418069.
16 J. J. Colin and H. F. Gaultier de Claubry, Mémoire sur les Combinaisons de l'Iode avec les Substances Végétales et Animales, *Ann. Chim.*, 1814, **90**, 87.
17 F. Stromeyer, Ein sehr empfindliches Reagens für Jodine, aufgefunden in der Stärke (Amidon), *Ann. Phys.*, 1815, **49**, 146.
18 S. Madhu, H. A. Evans, V. V. T. Doan-Nguyen, J. G. Labram, G. Wu, M. L. Chabinyc, R. Seshadri and F. Wudl, Infinite Polyiodide Chains in the Pyrroloperylene–Iodine Complex: Insights into the Starch–Iodine and Perylene–Iodine Complexes, *Angew. Chem., Int. Ed.*, 2016, **55**, 8032.
19 S. Wei, J. Wang, S. Deng, S. Zhang and Q. Li, Hypervalent iodine with linear chain at high pressure, *Sci. Rep.*, 2015, **5**, 14393.
20 W. Zhang, A. R. Oganov, Q. Zhu, S. S. Lobanov, E. Stavrou and A. F. Goncharov, Stability of numerous novel potassium chlorides at high pressure, *Sci. Rep.*, 2016, **6**, 26265.
21 N. N. Patel, A. K. Verma, A. K. Mishra, M. Sunder and S. M. Sharma, The synthesis of unconventional stoichiometric compounds in the K–Br system at high pressures, *Phys. Chem. Chem. Phys.*, 2017, **19**, 7996.
22 N. N. Patel, M. Sunder, A. B. Garg and H. K. Poswal, Pressure-induced polymorphism in hypervalent CsI3, *Phys. Rev. B*, 2017, **96**, 174114.

23 T. Poreba, S. Racioppi, G. Garbarino, W. Morgenroth and M. Mezouar, Investigating the Structural Symmetrization of CsI3 at High Pressures through Combined X-ray Diffraction Experiments and Theoretical Analysis, *Inorg. Chem.*, 2022, **61**, 10977.

24 Z. L. Li, Q. J. Li, H. Y. Li, L. Yue, D. L. Zhao, F. Tian, Q. Dong, X. T. Zhang, X. L. Jin, L. J. Zhang, R. Liu and B. B. Liu, Pressure-Tailored Band Engineering for Significant Enhancements in the Photoelectric Performance of CsI3 in the Optical Communication Waveband, *Adv. Funct. Mater.*, 2022, **32**, 2108636.

25 Y. Yin, A. Aslandukova, N. Jena, F. Trybel, I. A. Abrikosov, B. Winkler, S. Khandarkhaeva, T. Fedotenko, E. Bykova, D. Laniel, M. Bykov, A. Aslandukov, F. I. Akbar, K. Glazyrin, G. Garbarino, C. Giacobbe, E. L. Bright, Z. Jia, L. Dubrovinsky and N. Dubrovinskaia, Unraveling the Bonding Complexity of Polyhalogen Anions: High-Pressure Synthesis of Unpredicted Sodium Chlorides Na_2Cl_3 and Na_4Cl_5 and Bromide Na4Br5, *J. Am. Chem. Soc. Au*, 2023, **3**, 1634.

26 D. D. Wang, H. J. Zhang, W. W. Yu and Z. K. Tang, Thermal Evolution of One-Dimensional Iodine Chains, *J. Phys. Chem. Lett.*, 2017, **8**, 2463.

27 H.-P. Komsa, R. Senga, K. Suenaga and A. V. Krasheninnikov, Structural Distortions and Charge Density Waves in Iodine Chains Encapsulated inside Carbon Nanotubes, *Nano Lett.*, 2017, **17**, 3694.

28 S. S. Lobanov, J. A. Daly, A. F. Goncharov, X. J. Chan, S. K. Ghose, H. Zhong, L. Ehm, T. J. Kim and J. B. Parise, Iodine in Metal-Organic Frameworks at High Pressure, *J. Phys. Chem. A*, 2018, **122**, 6109.

29 A. A. Tonkikh, D. V. Rybkovskiy and E. D. Obraztsova, Charge-Induced Structure Variations of 1D-Iodine Inside Thin SWCNTs, *J. Phys. Chem. C*, 2023, **127**, 3005.

30 T. Poręba, M. Świątkowski and R. Kruszyński, Molecular self-assembly of 1D infinite polyiodide helices in a phenanthrolinium salt, *Dalton Trans.*, 2021, **50**, 2800.

31 Z. D. Liu, Z. Yao, M. G. Yao, J. Y. Lv, S. L. Chen, Q. J. Li, H. Lv, T. Y. Wang, S. C. Lu, R. Liu, B. Liu, J. Liu, Z. Q. Chen, B. Zou, T. Cui and B. B. Liu, High-pressure behavior of bromine confined in the one-dimensional channels of zeolite AlPO4-5 single crystals, *J. Chem. Phys.*, 2016, **145**, 124319.

32 B. Schmidt, B. Schröder, K. Sonnenberg, S. Steinhauer and S. Riedel, From Polyhalides to Polypseudohalides: Chemistry Based on Cyanogen Bromide, *Angew. Chem., Int. Ed.*, 2019, **58**, 10340.

33 P. Voßnacker, T. Keilhack, N. Schwarze, K. Sonnenberg, K. Seppelt, M. Malischewski and S. Riedel, From Missing Links to New Records: A Series of Novel Polychlorine Anions, *Eur. J. Inorg. Chem.*, 2021, 1034.

34 D. J. Haase, H. Steinfink and E. J. Weiss, The Phase Equilibria and Crystal Chemistry of the Rare Earth Group VI Systems. I. Erbium-Selenium, *Inorg. Chem.*, 1965, **4**, 538.

35 A. J. Klein Haneveld and F. Jellinek, The crystal structure of stoichiometric uranium ditelluride, *J. Less-Common Met.*, 1970, **21**, 45.

36 R. Gérardin and J. Aubry, Préparation et identification d'un nouveau compose binaire Li2Sb, *C. R. Seances Acad. Sci., Ser. C*, 1974, **278**, 1097.

37 P. Böttcher, Tellurium-Rich Tellurides, *Angew. Chem., Int. Ed. Engl.*, 1988, **27**, 759.

38 K. Stöwe, The phase transition of TlTe: Crystal structure, *J. Solid State Chem.*, 2000, **149**, 123.

39 K. Cao, X.-X. Qu, H. Jiang, Y.-H. Su, C. Zhang and G. Frapper, Pressure-induced novel stable stoichiometries in molybdenum–phosphorus phase diagrams under pressure, *J. Phys. Chem. C*, 2019, **123**, 30187.

40 Y. Fu, F. Li, X. H. Zhang, C. Wang, X. B. Liu and G. C. Yang, Pressure-induced YSe3 and Y3Se with charming structures and properties, *J. Alloys Compd.*, 2022, **923**, 166465.

41 K. X. Zhao, Q. Y. Wang, H. G. Li, B. Gao, S. B. Wei, L. Zhu, H. Y. Xu, H. Y. Liu and S. T. Zhang, Superconductivity in dense scandium-based phosphides, *Phys. Rev. B*, 2023, **108**, 174513.

42 G. Papoian and R. Hoffmann, Hypervalent Bonding in One, Two, and Three Dimensions: Extending the Zintl–Klemm Concept to Nonclassical Electron-Rich Networks, *Angew. Chem., Int. Ed.*, 2000, **39**, 2408.

43 J. H. Perlstein, Organic Metals-The Intermolecular Migration of Aromaticity, *Angew. Chem., Int. Ed. Engl.*, 1977, **16**, 519.

44 M. Kertész and F. Vonderviszt, Electronic Structure of Long Polyiodide Chains, *J. Am. Chem. Soc.*, 1982, **104**, 5889.

45 J. K. Burdett, *Chemical bonds: A dialog*, John Wiley and Sons, New York, 1997, pp. 95–96.

46 M. Motta, C. Genovese, F. J. Ma, Z.-H. Cui, R. Sawaya, G. K.-L. Chan, N. Chepiga, P. Helms, C. Jiménez-Hoyos, A. J. Millis, U. Ray, E. Ronca, H. Shi, S. Sorella, E. M. Stoudenmire, S. R. White and S. W. Zhang, Ground-State Properties of the Hydrogen Chain: Dimerization, Insulator-to-Metal Transition, and Magnetic Phases, *Phys. Rev. X*, 2020, **10**, 031058.

47 J. Hempelmann, P. C. Müller, L. Reitz and R. Dronskowski, Quantum Chemical Similarities of Bonding in Polyiodides and Phase-Change Materials, *Inorg. Chem.*, 2023, **62**, 20162.

48 K. Wade, *Electron deficient compounds*, Nelson, London, 1971.

49 H. H. Osman, A. Otero-de-la-Roza, A. Munoz, P. Rodríguez-Hernandez and F. J. Manjón, Electron-deficient multicenter bonding in pnictogens and chalcogens: Mechanism of formation, *J. Mater. Chem. C*, 2024, **12**, 10447.

50 H. H. Osman, P. Rodríguez-Hernández, A. Muñoz and F. J. Manjón, A Unified Theory of Electron-Rich and Electron-Deficient Multicenter Bonds in Molecules and Solids: A Change of Paradigms, *J. Mater. Chem. C*, 2025, **13**, 3774.

51 W. Grochala, R. Hoffmann, J. Feng and N. W. Ashcroft, The Chemical Imagination at Work in Very Tight Places, *Angew. Chem., Int. Ed.*, 2007, **467**, 3620.

52 L. Zhang, Y. Wang, J. Lv and Y. Ma, Materials discovery at high pressures, *Nat. Rev. Mater.*, 2017, **2**, 17005.

53 M. S. Miao, Y. H. Sun, E. Zurek and H. Q. Lin, Chemistry under high pressure, *Nat. Rev. Chem.*, 2020, **4**, 508.

54 G. L. Breneman and R. D. Willett, The crystal structure of cesium tribromide and a comparison of the Br^{3-} and I^{3-} systems, *Acta Crystallogr., Sect. B*, 1969, **25**, 1073.

55 J. Runsink, S. Swen-Walstra and T. Migchelsen, Refinement of the crystal structures of (C6H5) 4AsI3 and CsI3 at 20 °C and at–160 °C, *Acta Crystallogr., Sect. B*, 1972, **28**, 1331.

56 K.-F. Von Tebbe and U. Georgy, Die Kristallstruckturen von Rubidiumtriiodid und Thalliumtriiodid, *Acta Crystallogr., Sect. C: Cryst. Struct. Commun.*, 1986, **42**, 1675.

57 K.-F. Tebbe, B. Freckmann, M. Hörner, W. Hiller and J. Strahle, Verfeinerung der Kristallstruktur des ammoniumtriiodids, NH4I3, *Acta Crystallogr., Sect. C: Cryst. Struct. Commun.*, 1985, **41**, 660.

58 F. J. Manjón, H. H. Osman, M. Savastano and Á. Vegas, Electron-Deficient Multicenter Bonding in Phase Change Materials: A Chance for Reconciliation, *Materials*, 2024, **17**, 2840.

59 M. Wuttig, C.-F. Schön, J. Lötfering, P. Golub, C. Gatti and J.-Y. Raty, Revisiting the nature of chemical bonding in chalcogenides to explain and design their properties, *Adv. Mater.*, 2023, **35**, 2208485.

60 R. F. W. Bader, Atoms in molecules, *Acc. Chem. Res.*, 1985, **18**, 9.

61 R. Nelson, C. Ertural, J. George, V. L. Deringer, G. Hautier and R. Dronskowski, LOBSTER: Local orbital projections, atomic charges, and chemical-bonding analysis from projector-augmented-wave-based density-functional theory, *J. Comput. Chem.*, 2020, **41**, 1931–1940.

62 P. C. Müller, C. Ertural, J. Hempelmann and R. Dronskowski, Crystal orbital bond index: covalent bond orders in solids, *J. Phys. Chem. C*, 2021, **125**, 7959.

63 J. Hempelmann, P. C. Müller, C. Ertural and R. Dronskowski, The Orbital Origins of Chemical Bonding in Ge–Sb–Te Phase Change Materials, *Angew. Chem., Int. Ed.*, 2022, **61**, e202115778.

64 J. Hempelmann, P. C. Müller, L. Reitz and R. Dronskowski, Quantum Chemical Similarities of Bonding in Polyiodides and Phase-Change Materials, *Inorg. Chem.*, 2023, **62**, 20162.

65 H. H. Osman and F. J. Manjón, Chemical Bonding in Dense $A^{IV}X^{VI}$ and $A_2{}^{V}X_3{}^{VI}$ Chalcogenides: Electron-Deficient Multicenter Bonds in Electron-Rich Elements, *J. Mater. Chem. C*, 2025, **13**, 18780.

66 Á. M. Pendás and E. Francisco, Chemical Bonding from the Statistics of the Electron Distribution, *Chem. Phys. Chem.*, 2019, **20**, 2722.

67 B.-B. Zhang, X. Liu, B. Xiao, K. G. Gao, S.-T. Dong, Y. D. Xu, Y. C. He, J. Zhou and W. Q. Jie, Solution-grown hypervalent CsI3 crystal for high sensitive X-ray detection, *Phys. Status Solidi B*, 2020, **257**, 1900290.

68 M. Wuttig, V. L. Deringer, X. Gonze, C. Bichara and J.-Y. Raty, Incipient metals: functional materials with a unique bonding mechanism, *Adv. Mater.*, 2018, **30**, 1803777.

69 H. H. Osman, J. L. Rodrigo-Ramón, S. Ullah, E. Bandiello, D. Errandonea, Ó. Gomis, T. García-Sánchez, P. Botella, R. Oliva, P. Rodríguez-Hernández, A. Muñoz, C. Popescu, F. G. Alabarse and F. J. Manjón, Unconventional Electron-Deficient Multicenter Bonds in AIO3 Perovskites, *Chem. Mater.*, 2025, **37**, 4187–4202.

70 D. J. Haase, H. Steinfink and E. J. Weiss, The Phase Equilibria and Crystal Chemistry of the Rare Earth Group VI Systems. I. Erbium-Selenium, *Inorg. Chem.*, 1965, **4**, 538.

71 A. J. Klein Haneveld and F. Jellinek, The crystal structure of stoichiometric uranium ditelluride, *J. Less-Common Met.*, 1970, **21**, 45.

72 M. Sulli, A. Bianchi, C. Bazzicalupi and M. Savastano, 1D Iodine Chains: The Innocent Complexity of a Thread of Iodine Beads, *ChemRxiv*, 2025, DOI: **10.26434/chemrxiv-2025-fxl3p**.

73 H. K. Mao, J. Xu and P. M. Bell, Calibration of the ruby pressure gauge to 800 kbar under quasi-hydrostatic conditions, *J. Geophys. Res.*, 1986, **91**, 4673.

74 M. Wojdyr, Fityk: a general-purpose peak fitting program, *J. Appl. Crystallogr.*, 2010, **43**, 1126.

75 P. Hohenberg and W. Kohn, Inhomogeneous Electron Gas, *Phys. Rev. B*, 1964, **136**, 864.

76 G. Kresse and J. Furthmüller, Efficiency of ab-initio total energy calculations for metals and semiconductors using a plane-wave basis set, *Comput. Mater. Sci.*, 1996, **6**, 15.

77 G. Kresse and J. Furthmüller, Efficient iterative schemes for ab initio total-energy calculations using a plane-wave basis set, *Phys. Rev. B: Condens. Matter Mater. Phys.*, 1996, **54**, 11169.

78 P. E. Blöchl, Projector augmented-wave method, *Phys. Rev. B: Condens. Matter Mater. Phys.*, 1994, **50**, 17953.

79 D. Joubert, G. Kresse and D. Joubert, From ultrasoft pseudopotentials to the projector augmented-wave method, *Phys. Rev. B: Condens. Matter Mater. Phys.*, 1999, **59**, 1758.

80 J. P. Perdew, K. Burke and M. Ernzerhof, Generalized gradient approximation made simple, *Phys. Rev. Lett.*, 1996, **77**, 3865.

81 S. Grimme, S. Ehrlich and L. Goerigk, Effect of the damping function in dispersion corrected density functional theory, *J. Comput. Chem.*, 2011, **32**, 1456.

82 H. J. Monkhorst and J. D. Pack, Special points for Brillouin-zone integrations, *Phys. Rev. B*, 1976, **13**, 5188.

83 K. Parlinski, Z. Q. Li and Y. Kawazoe, First-Principles Determination of the Soft Mode in Cubic ZrO2, *Phys. Rev. Lett.*, 1997, **78**, 4063.

84 P. Giannozzi, O. Andreussi, T. Brumme, O. Bunau, M. Buongiorno Nardelli, M. Calandra, R. Car, C. Cavazzoni, D. Ceresoli, M. Cococcioni, N. Colonna, I. Carnimeo, A. Dal Corso, S. de Gironcoli, P. Delugas, R. A. DiStasio, A. Ferretti, A. Floris, G. Fratesi, G. Fugallo, R. Gebauer, U. Gerstmann, F. Giustino, T. Gorni, J. Jia, M. Kawamura, H.-Y. Ko, A. Kokalj, E. Küçükbenli, M. Lazzeri, M. Marsili, N. Marzari, F. Mauri, N. L. Nguyen, H.-V. Nguyen, A. Otero-de-la-Roza, L. Paulatto, S. Poncé, D. Rocca, R. Sabatini, B. Santra, M. Schlipf, A. P. Seitsonen, A. Smogunov, I. Timrov, T. Thonhauser, P. Umari, N. Vast, X. Wu and S. Baroni, Advanced capabilities for materials modelling with Quantum ESPRESSO, *J. Phys.: Condens. Matter*, 2017, **29**, 465901.

85 A. A. Mostofi, J. R. Yates, Y.-S. Lee, I. Souza, D. Vanderbilt and N. Marzari, wannier90: A tool for obtaining maximally-localised Wannier functions, *Comput. Phys. Commun.*, 2008, **178**, 685.

86 A. Otero-de-la-Roza, E. R. Johnson and V. Luaña, Critic2: A program for real-space analysis of quantum chemical interactions in solids, *Comput. Phys. Commun.*, 2014, **185**, 1007.
87 A. Dal Corso, Pseudopotentials periodic table: From H to Pu, *Comput. Mater. Sci.*, 2014, **95**, 337.
88 A. Otero-de-la-Roza, Á. Martín Pendás and E. R. Johnson, Quantitative electron delocalization in solids from maximally localized Wannier functions, *J. Chem. Theory Comput.*, 2018, **14**, 4699.
89 P. Vinet, J. R. Smith, J. Ferrante and J. H. Rose, Temperature effects on the universal equation of state of solids, *Phys. Rev. B: Condens. Matter Mater. Phys.*, 1987, **35**, 1945.
90 F. Birch, Elasticity and constitution of the Earth's interior, *J. Geophys. Res.*, 1952, **57**, 227.
91 R. C. L. Mooney Slater, The Triiodide Ion in Tetraphenyl Arsonium Triiodide, *Acta Crystallogr.*, 1959, **12**, 187.
92 J. C. Slater, Note on the interatomic spacings in the ions, I^{3-}, FHF–, *Acta Crystallogr.*, 1959, **12**, 197.
93 E. Kroumova, M. Aroyo, J. Perez-Mato, A. Kirov, C. Capillas, S. Ivantchev and H. Wondratschek, Bilbao crystallographic server: useful databases and tools for phase-transition studies, *Phase Transitions*, 2003, **76**, 155.
94 P. Deplano, J. R. Ferraro, M. L. Mercuri and E. F. Trogu, Structural and Raman spectroscopic studies as complementary tools in elucidating the nature of the bonding in polyiodides and in donor-I2 adducts, *Coord. Chem. Rev.*, 1999, **188**, 71.

